Ukrainian Journal of Ecology

Ukrainian Journal of Ecology, 2021, 11(4), 18-29, doi: 10.15421/2021_194

ORIGINAL ARTICLE

Pathological and pathohistological characteristics of African swine fever in the western region of Ukraine

O. Shchebentovska[1], O. Zaytsev[1],A. Tybinka[1],O. Lozhkina[2],M. Kupnevska[2], S. Lytvynenko[2]

[1]Stepan Gzhytskyi National University of Veterinary Medicine and Biotechnologies
50 PekarskaSt., Lviv, 79010, Ukraine
[2]State Scientific and Research Institute of Laboratory Diagnostics and Veterinary and Sanitary Expertise
30 Donetska St., Kyiv, 03151, Ukraine
**Corresponding author E-mail: schebentovskaolga@gmail.com*

Received: 28.04.2021. Accepted: 11.06.2021.

African swine fever is one of the most severe transboundary diseases, included in the list of dangerous animal diseases (TAD) identified by EMPRES (Emergency Prevention System for Transboundary Animals and Plant Pests and Diseases). This disease causes significant damage to the economy, trade, and food security of various countries and can quickly spread from one country to another, reaching the scale of epizooty. The ASF (African swine fever) virus is a pantropic one with a selective effect on lymphoid cells and vascular endothelium. After the virus enters the body through the blood and lymphatic vessels, it reproduces in sensitive cells. A cytopathic effect accompanies the process on leukocytes, macrophages, and endothelial cells. The article describes the clinical picture, pathological and histological changes in various organs of pigs during the acute progression of ASF. The following manifestations characterize the clinical manifestations of the disease: a temperature increase up to 42°C, skin cyanosis of the ears and abdomen, shortness of breath, arrhythmia, diarrhea with blood impurities, and partial paresis. Postmortem changes developed quite rapidly. The pathological autopsy revealed bloody discharge from natural openings, serous infiltrates in the subcutaneous and intermuscular connective tissue, splenomegaly, hemorrhagic lymphadenitis, multiple spot hemorrhages in the parenchyma of the kidneys and liver, serous edema of the gallbladder wall, pulmonary edema and hemorrhagic pneumonia, hemorrhage in the endocardium, and heart valves. Morphologically, diffuse karyorrhexis of lymphocytes, necrosis of lymphoid nodules, and diffuse lesion of blood vessel walls were found in the spleen of pigs. Alternative serous hemorrhagic lymphadenitis was detected in the lymph nodes. There was a massive infiltration of interparticle connective tissue by histiocytes, lymphocytes, and plasma cells in the liver. Membrane glomerulonephritis, granular hyaline drop dystrophy of the distal and proximal tubules' epithelium with the formation of hyaline cylinders were found in the kidneys.

Keywords: cyanosis of the skin, splenomegaly, hemorrhagic lymphadenitis, hemorrhagic pneumonia, edema, erythrodiapedesis, lymphocytic karyorrhexis, membranous glomerulonephritis.

Introduction

African swine fever (ASF) causes significant economic damage not only to West African countries but also to the European ones. It is one of the most transboundary severe diseases due to the high mortality rate and lack of vaccines and proper treatments (Blome et al., 2013; Beltrán-Alcrudo et al., 2017; Pautienius et al., 2018). At the beginning of 2019, according to official OIE reports, ASF was registered in China and Vietnam, the leading pig breeding countries. Analysts expect it could lead to severeconsequences for global food security (Ge et al., 2018; Sunwoo et al., 2019). At the FAO World Symposium in 2019, Chinese scientists discussed the need to detect the disease early. They focused on the research of pathogen transmission ways (namely, the analysis of contact surfaces on which the virus retains its viability for quite a long time), vehicle control, and tools that could come into contact with sick animals and be a source of virus spread (Beltran-Alcrudo et al., 2019; Kim et al., 2019; Flannery et al., 2020). The presented report indicated that PCR tests for the ASF virus in feed and raw materials selected from Chinese feed mills had yielded many positive results (Dee et al., 2018). About 22% of positive tests were obtained from vehicles moving between farms, 15% from feedstock, 7% from feed ingredients, and 5% from feed (Faostat, 2019). That is why measures to prevent disease spread should be aimed at identifying contaminants.

In Ukraine, the speed and range of the ASF virus are caused primarily by the dynamic development of industrial pig farming and individual homesteads and the intensive movement of people and animal products from one region to another. Disorganization and insecurity of marketing systems that do not provide incentives for producers to invest funds in improving pig farming are also of great importance. This is especially true for small farms with a low level of biosecurity. According to the official reports of the State Food and Consumer Service of Ukraine in 2020, ASF outbreaks were detected in individual homesteads in Sumy and Zaporizhia region. In April 2020, an outbreak of the disease was registered among wild boars in the hunting grounds of Tulchyn district in the Vinnytsia region. In March 2020, there was an outbreak in individual homestead in Kirovohrad and Kherson region; in February 2021 - in an individual homestead in the Vinnytsia region. However, official statistics do not always reflect the actual epizootiological situation, since veterinary specialists cannot control all private farms where pigs have died or have been slaughtered. It's also

difficult to stop the migration of wild boars through forests and border areas between Ukraine, Belarus, Russia, or Poland (Pejsak et al., 2014; Sánchez-Vizcaíno et al., 2015; Makarov, 2018). Therefore, early detection of the infection source and holding timely measures to prevent the spread of the virus remain extremely relevant (De la Torre et al., 2015; Cwynar et al., 2019; Mazloum et al., 2019).

ASF virus is a double-stranded DNA with a 4-layer lipoprotein shell. It contains 28 to 34 structural proteins, induces the formation of about 95-111 infectious proteins, and belongs to the Asfarviridae family (Tulman et al., 2009; Galindo et al., 2017). Spherical virions have 175-215 nm in diameter. After the virus enters the body through the blood and lymphatic vessels, it reproduces in sensitive cells, which is manifested by a cytopathic effect on leukocytes, macrophages, and endothelial cells (Dixon et al., 2013). It results in the necrosis of blood vessel endothelial cells, disorganization of small vessels' connective tissue structures, and total karyorrhexis of lymphocytes with the release of large amounts of virus into the blood (Ezema et al., 2011). The main manifestations of the disease include sharp hyperemia, enlargement of regional lymph nodes where an increased proliferation of lymphocytes and macrophages occurs, and the sharp increase in the number of eosinophils (Gómez-Villamandos et al., 2013; Zakaryan et al., 2015). Clinical signs of the disease in pigs are quite different and depend on the virus virulence, the epizootic situation in the region, the breed of pigs, and infection routes (Galindo et al., 2017; Pejsak et al., 2018). The ASF virus has isolates with high, medium, and low virulence (Blome et al., 2013). Therefore, the control of ASF is of great social and economic importance, especially in terms of international animal trade and products of animal origin (Mur et al., 2012).

The development of ASF clinical signs and the main pathological changes have been described mainly in the studies of foreign scientists, where the pathology of hematopoietic organs is highlighted in much detail (Sanchez-Cordon et al., 2008, 2019; Rodríguez-Bertos et al., 2020; Salguero et al., 2020). In Ukraine, studies on episodically described macroscopic changes in the lymphoid organs of pigs have also been published. However, a comprehensive pathohistological examination of all organs in a confirmed ASF case has not been found among the available domestic references. Therefore, our work aims to describe in detail the clinical picture, pathological and histological changes in various organs of pigs during the acute ASF progression cases detected at the farm Halychyna-Zakhid LLC in the Lviv region.

Materials and Methods

Material for the study was selected from dead and forcibly slaughtered pigs at Halychyna-Zakhid LLC (72.5 thousand pigs), located in Kavske village, Stryi district, Lviv region. Here, on August 15, 2019, the first case of ASF was recorded. During the night of 15 to August 16, about 150 adult pigs fell ill, demonstrating the following clinical manifestations: temperature of 41-42°C, cyanosis of the ears and abdomen, skin, shortness of breath, arrhythmia, diarrhea with blood, and partial paresis.

Bloody discharge from the snout, cough, and lethargy was also observed. The animals gathered in small groups of 8-10 pigs. Clinical manifestations of the disease were first observed in a single technological room. They became widespread after 5-6 days and finally covered the entire farm. From 60 to 100 pigs died each subsequent 24 hours. Four days later, 350 sows with similar clinical signs fell ill. To make a diagnosis, a biomaterial was prepared for PCR diagnostics, and pathological autopsy of animals with the selection of organs and tissues for electron microscopic and histopathological examination was performed. The biomaterial was sent to the State Research Institute for Laboratory Diagnostics and Veterinary Sanitary Examination (Kyiv) and Lviv Regional State Laboratory of Veterinary Medicine. A positive result, i.e., confirmation of ASF, was received on August 17, 2019.

Fragments of internal organs were selected for histological examination and fixed in 10% solution of neutral formalin and Carnua-Buen fluid. The tissues were compacted, dehydrated, and poured into paraffin according to the conventional methods. Histocuts with a thickness of 7 μm were made from paraffin blocks using a sled microtome MS-2. Paraffin sections were stained with hematoxylin and eosin, and the McManus PAS reaction was performed (Kiceli, 1962; Merkulov, 1969). Photo fixation of histological specimens was performed using Leica DM-2500 microscope, Leica DFC 450-C camera, and Leica Application Suite Version 4.4 software.

The spleen and lymph nodes were taken from the forcibly slaughtered pigs to perform electron microscopic examination. To prepare the ultrathin sections, fragments of organs were fixed in a Millonig fixative with a pH of 7.36 at the temperature of melting ice and dehydrated in ethyl alcohols of increasing concentration. Furthermore, the fragments were kept in propylene oxide and poured into a mixture of epon and araldite. The polymerization was carried out in a thermostat at a temperature of 60°C for 24 hours. Ultrathin sections were made from the obtained blocks and mounted on support grids, which were contrasted using Reynolds' lead citrate and uranyl acetate (Uikli, 1975). Ultrathin sections were viewed and photographed in a Tesla BS-500 transmission electron microscope under an accelerating voltage of 60 kV. Photo fixation was performed using FT-41P film. After processing the film, the obtained negatives were digitized using an Epson Perfection V500 photo scanner and its software package.

Results and Discussion

The pathological autopsy revealed that the carcasses of dead pigs were well fed, not depleted (Fig. 1); cadaveric numbness was pronounced. Postmortem changes developed quite rapidly. The skin around the ears, eyes, submandibular space, chest, and hip surfaces were cherry-colored (Fig. 1-3). There were bloody discharges from natural openings (Fig. 4). Internal examination showed serous infiltrates around the lymph nodes in the subcutaneous and intermuscular connective tissue. Serous-hemorrhagic exudate of the yellowish-red color was found in the pericardial, thoracic, and abdominal cavities. The most characteristic changes were detected in the spleen, lymph nodes, and kidneys. The spleen was 2-4 times larger, the color varied from dark cherry to black (Fig. 5 and 6), the capsule was elastic, and the organ's pulp was softened, permeated with blood. Submandibular, thoracic, superficial cervical, inguinal, mesenteric, and gastric lymphatic nodes were sharply increased, intensively blood-filled, and of dark red color on a section surface (Fig. 7-11). The kidneys were enlarged, infused with blood with multiple spot hemorrhages in both cortex and renal pelvis. The renal pelvis walls were thickened due to edema and hemorrhagic infiltration (Fig. 12-14). In the bladder, the redness of the mucous membrane was found. Diapedetic hemorrhage also occurred in some animals.

Fig. 1. Cyanosis of the skin in the area of the chest and abdomen.

Fig. 2. Cyanosis of the skin in the area of ears (1) and neck (2).

Fig. 3. Cyanosis of the skin on the hip surface.

Fig. 4. Bloody discharge from the nasal cavity.

Fig. 5. Enlarged spleen (splenomegaly).

Fig. 6. Spleen (splenomegaly (1), rounded edges, tense capsule).

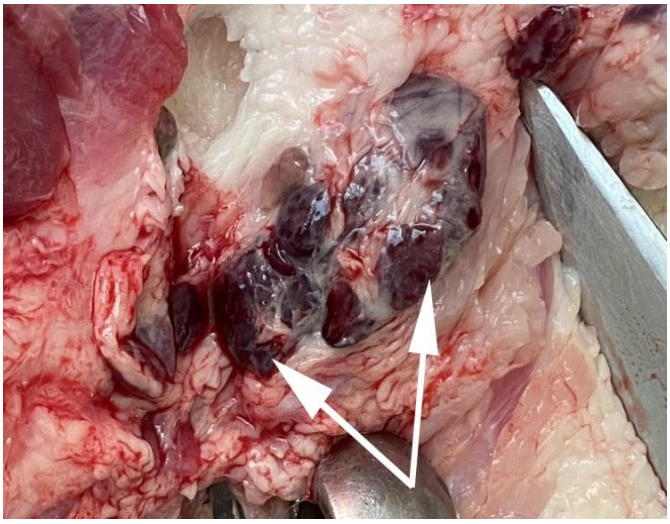

Fig. 7. Superficial cervical lymph nodes. Hemorrhagic lymphadenitis.

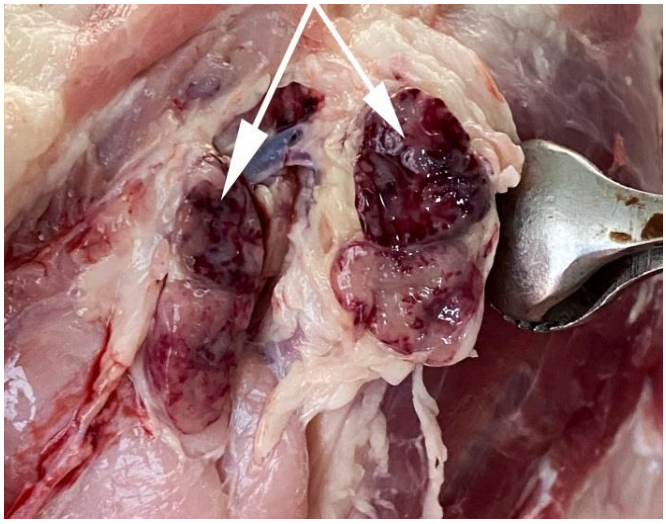

Fig. 8. Hemorrhagic lymphadenitis of the thoracic lymph nodes.

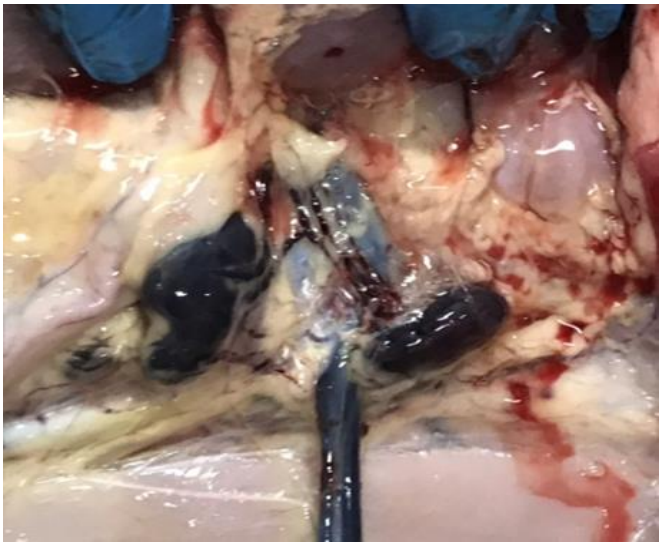

Fig. 9. Inguinal lymph nodes. Hemorrhagic lymphadenitis.

Fig. 10. Mesenteric lymph nodes. Serous lymphadenitis.

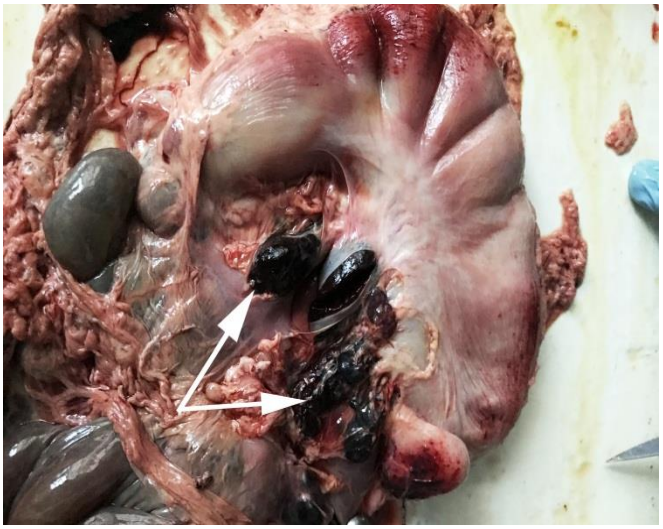

Fig. 11. Hemorrhagic lymphadenitis of gastric lymph nodes.

Fig. 12. Kidney. Diffuse punctate hemorrhage under the capsule.

Fig. 13. A sharp increase in the kidney. Diffuse hemorrhage under the capsule.

Fig. 14. Multiple hemorrhages into the cortical substance of the kidney (1).

The mucous membranes of the nasal cavity, larynx, and trachea were swollen with small dot hemorrhages. The nasal cavity, larynx, trachea, and bronchi were filled with foamy fluid and red mucus. The lungs were full-blooded and dark red. Areas with multiple punctate hemorrhages were found under the pulmonary pleura, a significant amount of blood was excreted from the lung parenchyma section, and foamy fluid accumulated in the trachea and bronchi (Fig. 15). The mediastinal lymph nodes were enlarged of the dark cherry color (Fig. 16). There were diffuse petechial hemorrhages on the aorta's outer wall (Fig. 16).

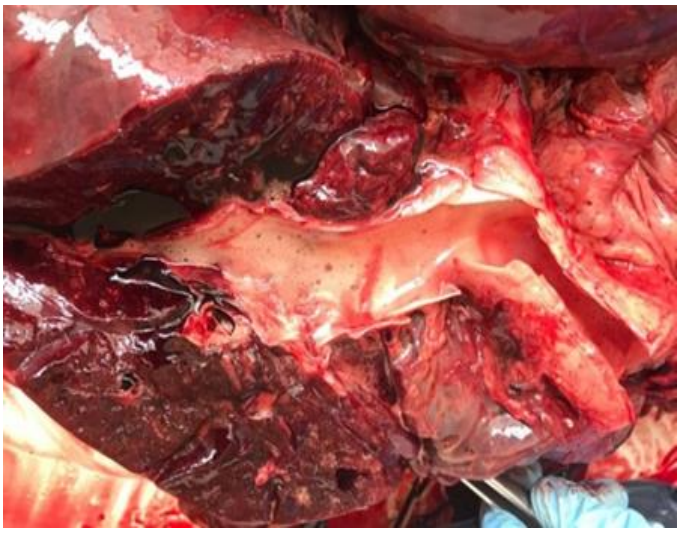

Fig. 15. Hemorrhagic pneumonia and pulmonary edema, foamy exudate with blood in the lumen of the bronchus.

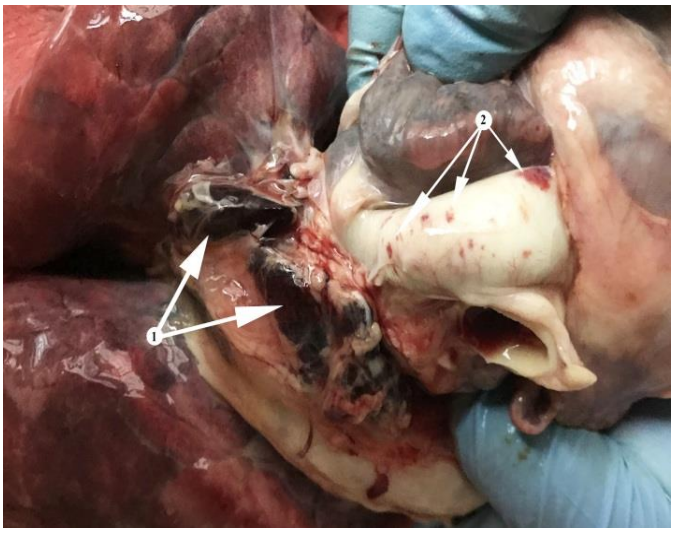

Fig. 16. Hemorrhagic lymphadenitis of the mediastinal lymph nodes (1). Petechial hemorrhage on the outer wall of the aorta (2).

The heart was enlarged, the heart muscle was flabby, dull in color, and blood vessels were filled. There were hemorrhages of various shapes and sizes under the epicardium, endocardium, and the heart ears (Fig. 17 and 18). Gastrointestinal tract changes were quite diverse and depended on the course of the disease. The mesentery was slightly swollen due to impregnation with serous exudate; the vessels were sharply filled with blood. The gastric mucosa was swollen with diffuse hemorrhage. Ecchymosis and petechial hemorrhages are visualized in the small intestine (Fig. 19). Wall edema with diapedetic hemorrhage in the mucosa was found in the cecum and colon. The liver was enlarged due to its strong blood supply, inhomogeneously colored with subcapsular hemorrhage, the edges were rounded (Fig. 20). The gallbladder was filled with thick, viscous bile of yellow-green color, sometimes with impurities of blood. Its walls were in a state of serous edema (Fig. 21), and the mucous membrane was dark brown. Electron microscopic examination of lymph nodes revealed ASF virus vibrio (Fig. 22).

Fig. 17. Spot hemorrhages on the epicardium.

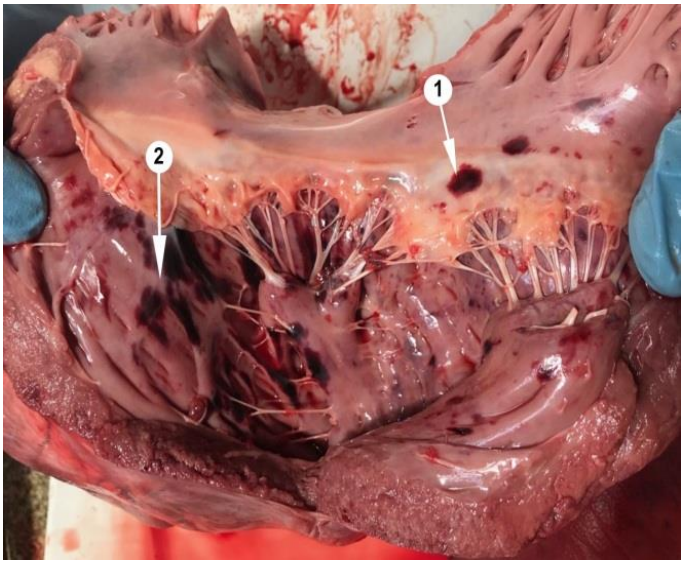

Fig. 18. Hemorrhages on the endocardium (2), hemorrhages on the valve (1).

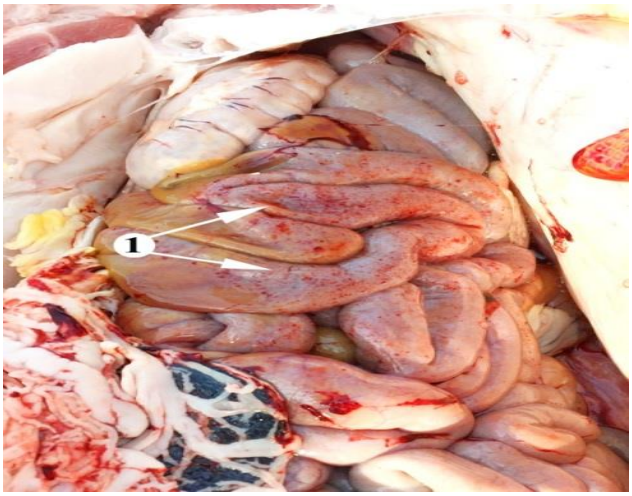

Fig. 19. Echimosal hemorrhage under the serous membrane of the small intestine (1).

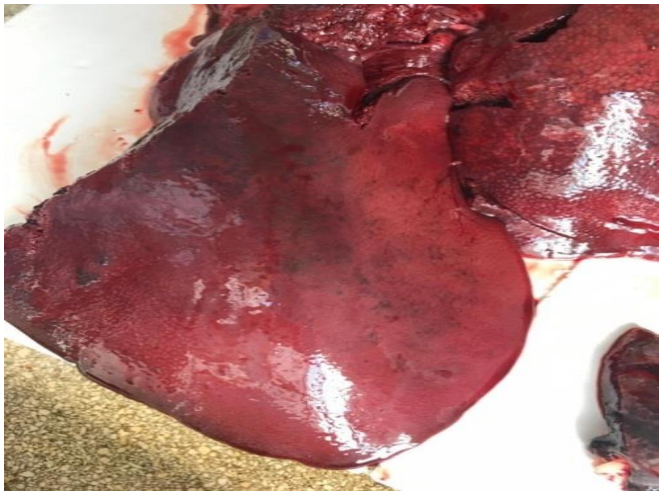

Fig. 20. Enlarged and unevenly colored liver with subcapsular hemorrhage.

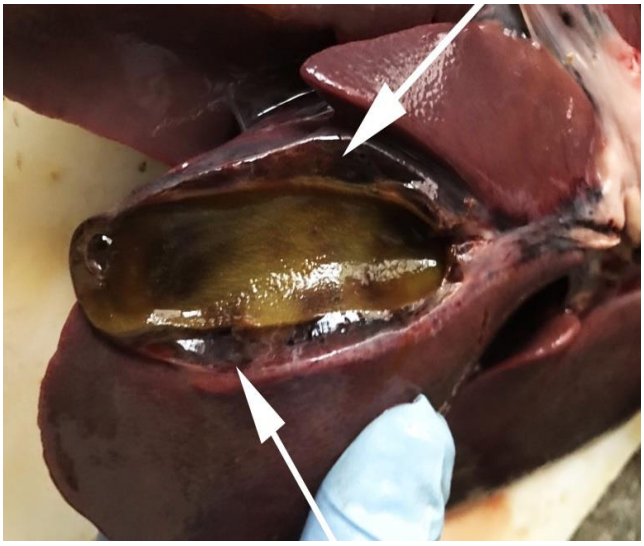

Fig. 21. Swelling of the gallbladder wall.

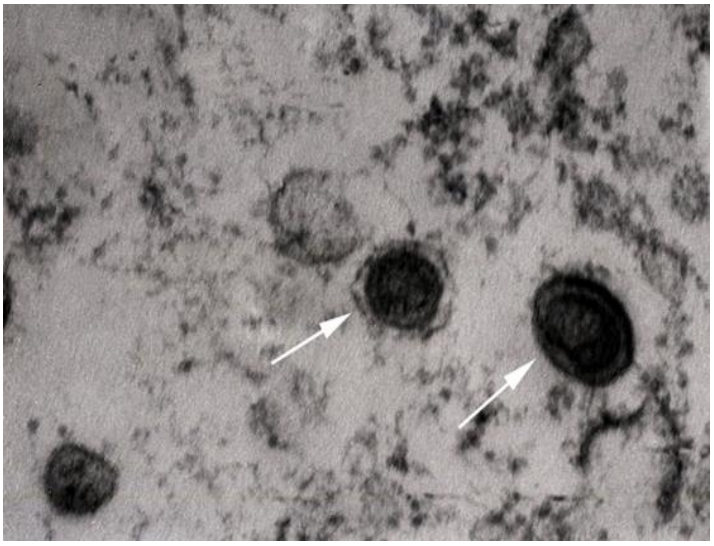

Fig. 22. Virions of ASF virus. Transmission electron microscopy. x 60 000.

Diffuse karyorrhexis of lymphocytes with the formation of significant areas of necrosis in lymphoid nodules and red pulp was detected optically in the spleen of pigs (Fig. 23 and 24). Characteristic features included eosinophilia, especially in areas of necrosis, diffuse infiltration of the pulp by erythrocytes (Fig. 25), lesions of blood vessel walls with endothelial cell dystrophy, and edema (Fig. 26), and necrosis of reactive centers of lymphoid nodules (Fig. 27 and 28). The lymph nodes were also characterized by acute venous stasis, erythrodiapedesis, hemorrhage (Fig. 29), alternative serous-hemorrhagic lymphadenitis, lymphocytic karyopyknosis, karyorrhexis, and necrosis of lymph nodes (Fig. 30).

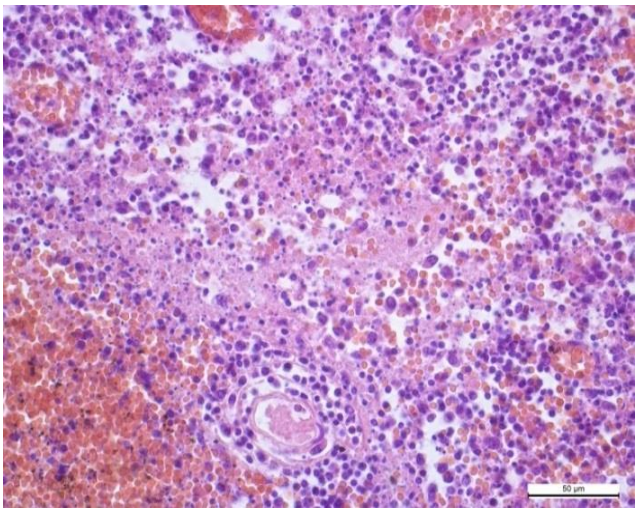

Fig. 23. Spleen. Karyopyknosis, karyorrhexis of lymphocytes, necrosis of lymphoid nodule. Hematoxylin and eosin. 400x.

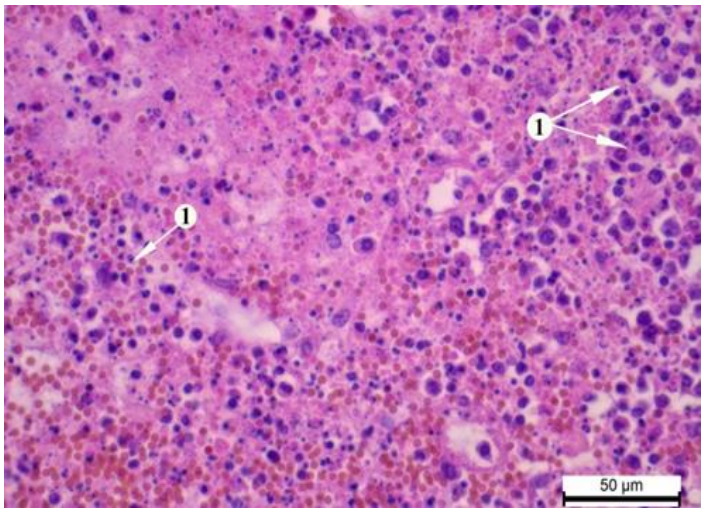

Fig. 24. Spleen. Karyopyknosis, karyorrhexis of lymphocytes (1), necrosis. Hematoxylin and eosin. 400x.

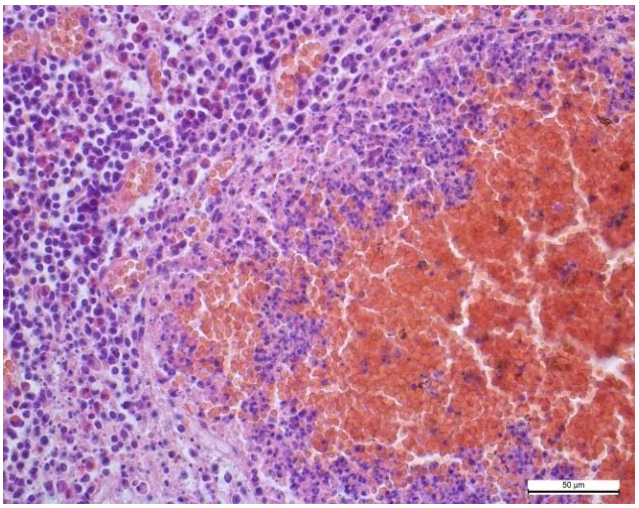

Fig. 25. Spleen. Diffuse infiltration of the pulp by erythrocytes. Hematoxylin and eosin. 400x.

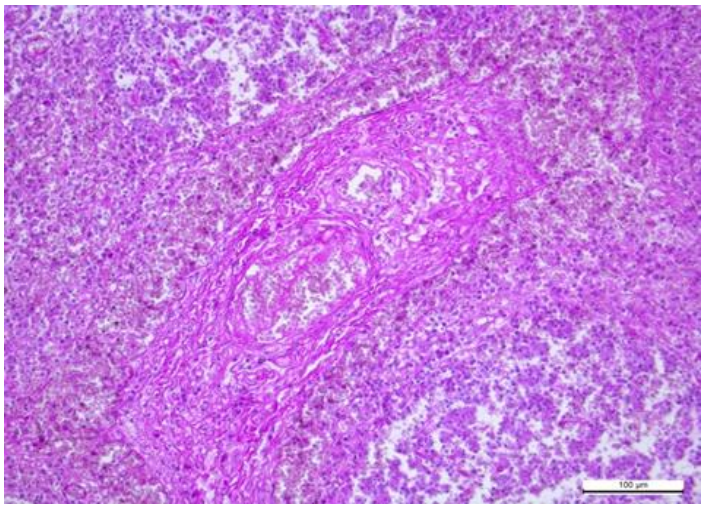

Fig. 26. Spleen. Defibering of vessel walls. Prevascular edema. PAS reaction. 200x.

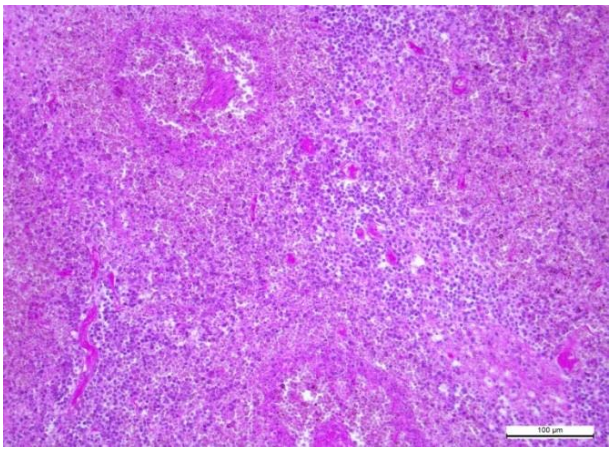

Fig. 27. Spleen. Necrosis of the reactive centers of lymphoid nodules. PAS reaction. 200x.

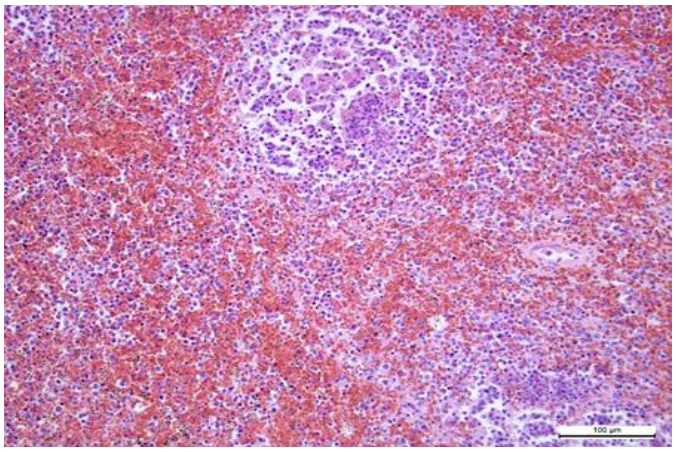

Fig. 28. Spleen. Necrosis of the reactive centers of lymphoid nodules. Hematoxylin and eosin. 200x.

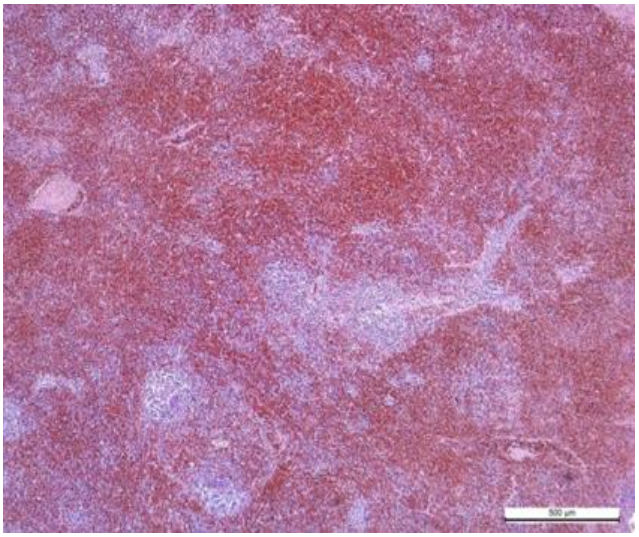

Fig. 29. Lymph node. Acute venous stasis. Hematoxylin and eosin. 100x.

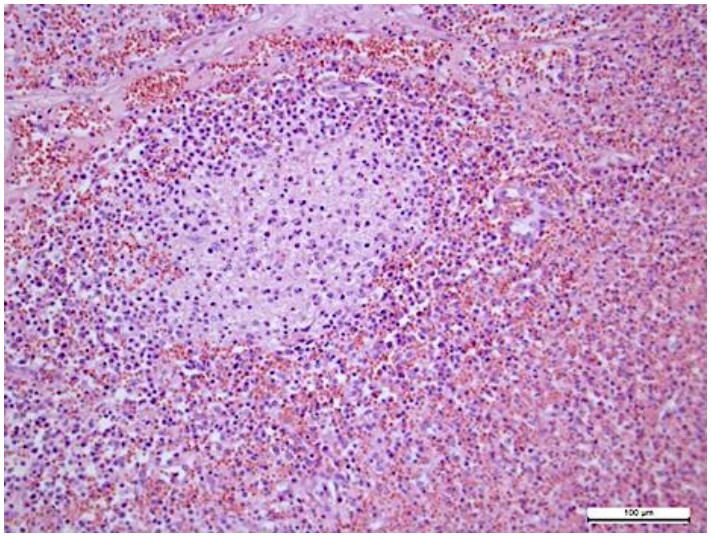

Fig. 30. Lymph node. Lymph node necrosis, erythrodiapedesis. Hematoxylin and eosin. 200x.

Histologically, acute vascular disorders were detected in the liver of pigs with ASF. They include stasis, perivasal edema, diapedetic hemorrhage, granular dystrophy of hepatocytes, necrosis of Kupffer cells. The interparticle connective tissue was swollen, massively infiltrated with lymphocytes, histiocytes, and macrophages (Fig. 31). The intraparticle hemocapillaries were full of blood; the beam structure was disturbed (Fig. 32). The cytoplasm of hepatocytes was somewhat granular, the nuclei of some hepatocytes were preserved and well visible. The cytoplasm of some hepatocytes was in a state of lysis.

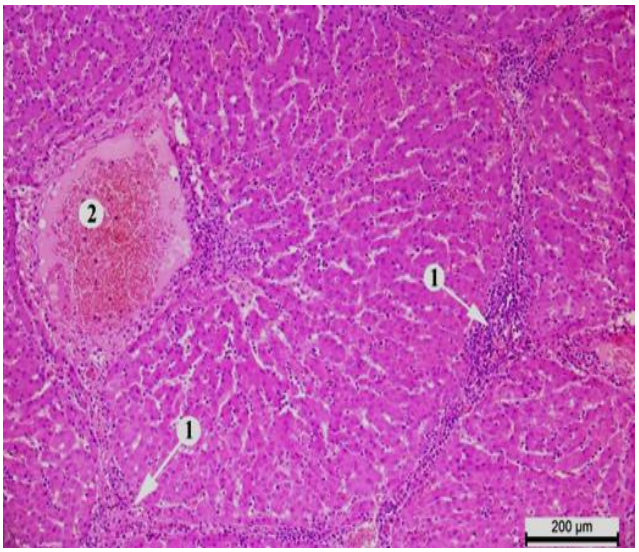

Fig. 31. Liver. Infiltration of interparticle connective tissue by histiocytes, lymphocytes, and plasma cells (1). Acute venous stasis (2). Hematoxylin and eosin. 100x.

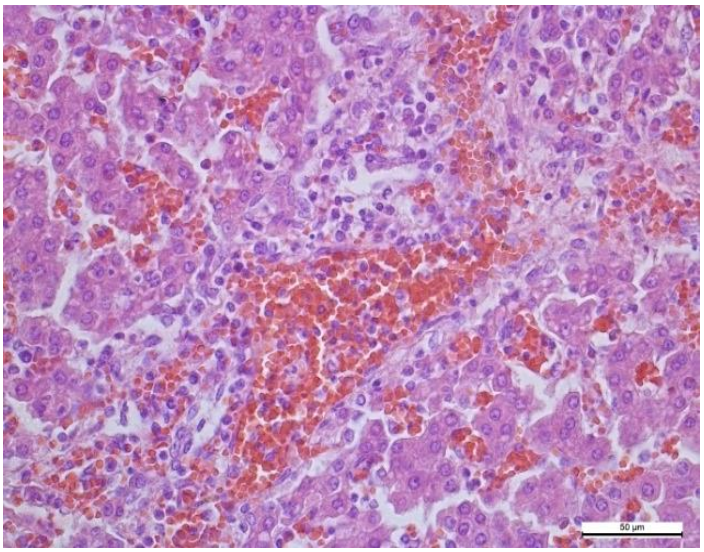

Fig. 32. Liver. Dilation of intraparticle capillaries, overflow with blood, and infiltration by histiocytes. Hematoxylin and eosin. 400x.

Microscopically, intense vascular blood supply, serous hemorrhagic pneumonia with severe circulatory disorders, and interstitial connective tissue edema were found in the lungs of pigs (Fig. 33). The lumens of the large and small bronchi were filled with erythrocytes and leukocytes. Alveolar lumens contained a homogeneous, light pink edematous fluid (Fig. 34). The capillaries were dilated, and erythrocytes were sometimes visible in the lumens of the alveoli. There was erythrocyte and leukocyte infiltration of the interstitium. Erythrocyte infiltration was expressed in the layers of lobular connective tissue; the alveoli walls were swollen, filled with erythrocytes.

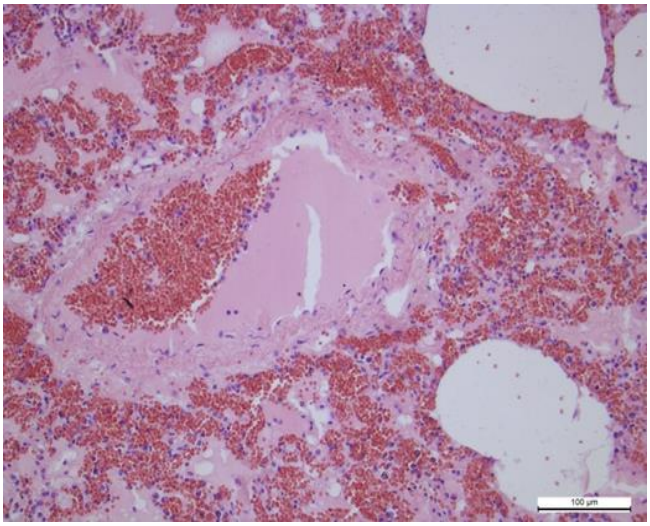

Fig. 33. Lungs. Perivascular edema. Dilated vessels filled with erythrocytes and exudate. Hematoxylin and eosin. 400x.

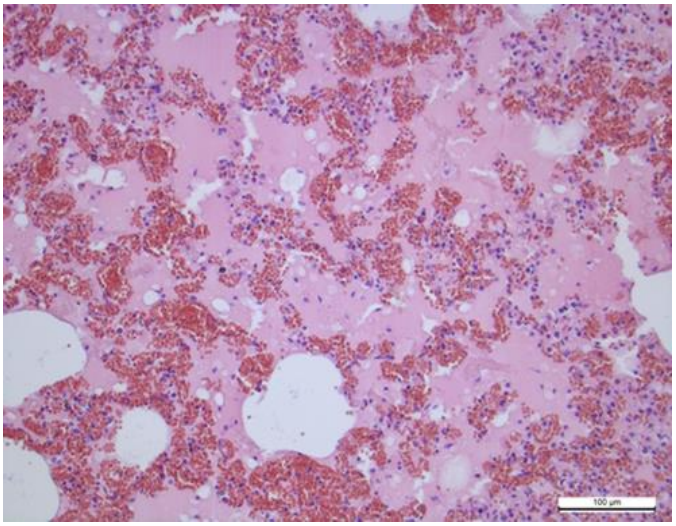

Fig. 34. Lungs. Dilated interalveolar septa filled with erythrocytes. Edematous fluid is in the alveoli. Hematoxylin and eosin. 200x.

Pathohistological examination of pig kidneys revealed membranous glomerulonephritis, granular and hyaline drop dystrophy of the epithelium of the distal and proximal tubules with the formation of hyaline cylinders.

The optical glomerular basement membrane of the renal corpuscles was unevenly thickened, the intercapillary spaces of the vascular glomeruli were dilated due to the accumulation of PAS-positive material in these places, the proliferation of mesangial cells and leukocyte infiltrates were sometimes noted (Fig. 35). The Shumlyansky-Bowman capsule of renal corpuscle was unevenly thickened. Accumulation of PAS-positive substances was noted on the surface of the parietal leaf of the capsule (Fig. 36).

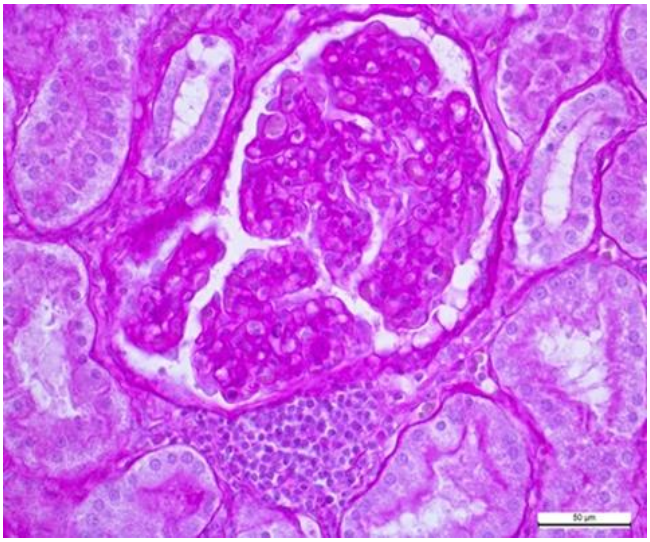

Fig. 35. Lymphoid infiltration of the glomerulus. PAS reaction. 400x.

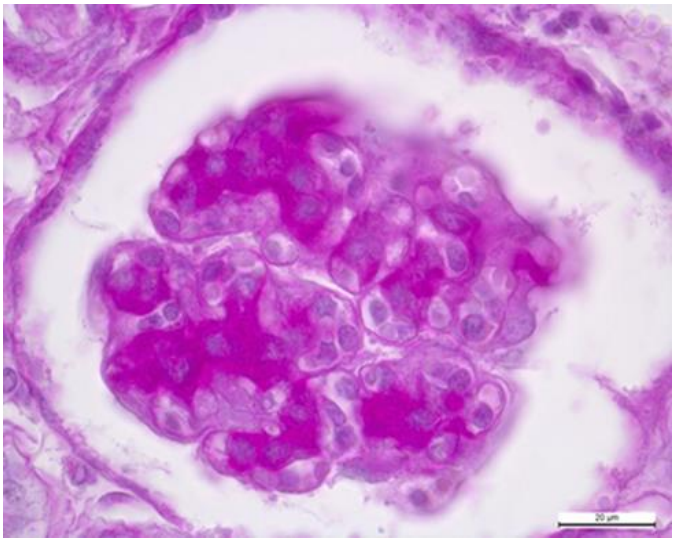

Fig. 36. Membrane glomerulonephritis. Diffuse thickening of the capillaries' basement membrane. Accumulation (formation) of PAS-positive subepithelial deposits. PAS reaction. x 900.

The tubular epithelium of the tubules was slightly deformed. Granular and hyaline-drop dystrophy and edema of the stroma were revealed in the proximal and distal tubules (Fig. 37). The cytoplasm of epitheliocytes of tortuous proximal tubules was swollen and granular, the borders of the cells were not always visible and apparent (Fig. 38). In some places, compaction of epithelial cells covering the proximal segment of the nephron was observed. Edema and granularity of the cytoplasm of nephrothelial cells were also detected in the distal tubules of the nephron. Homogeneous protein cylinders were found in the lumen of the tubules. With the progression of the disease, the accumulation of the matrix and the development of sclerosis were observed. Fibrinoid swelling and necrosis occurred in blood vessels (Fig. 39-42).

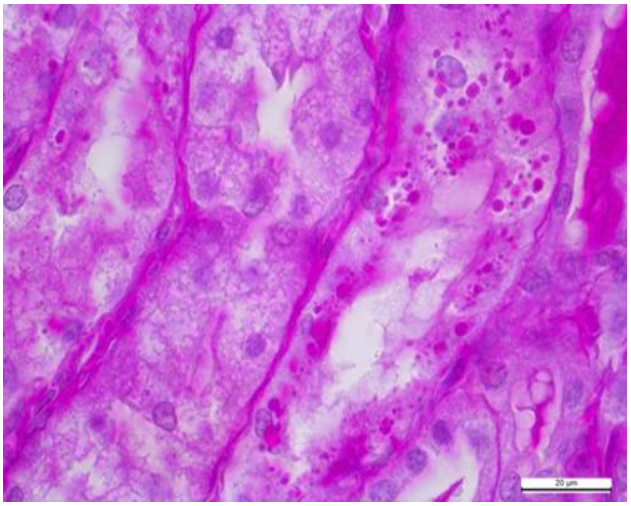

Fig. 37. Proximal tortuous tubules. Hyalin-drip dystrophy. PAS reaction. x 900.

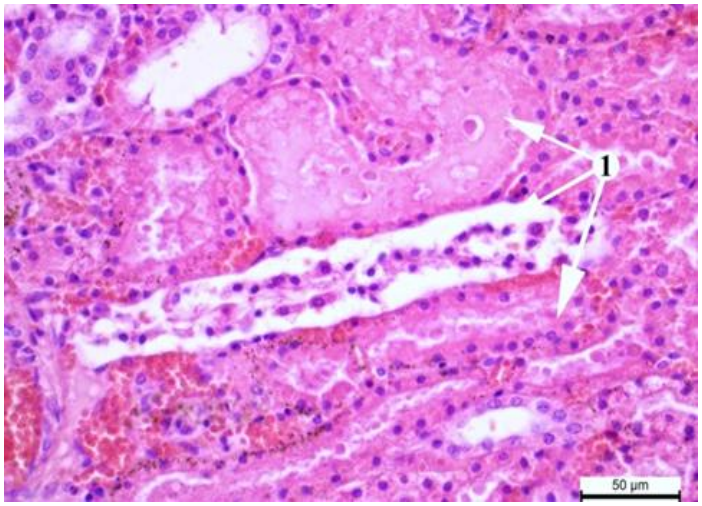

Fig. 38. Kidney. Necrosis of nephrotheliocytes of the distal tubules (1). Hematoxylin and eosin. 400.

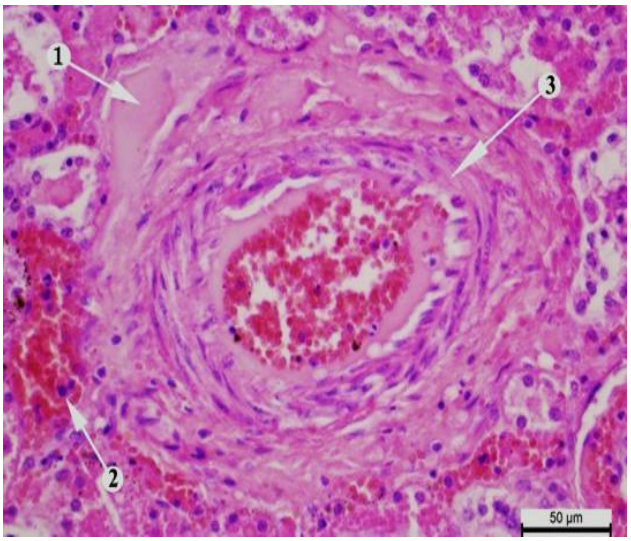

Fig. 39. Kidney. Perivasal edema (1), vacuolar dystrophy of endothelial cells (3). Erythrodiapedesis (2). Hematoxylin and eosin. 400x.

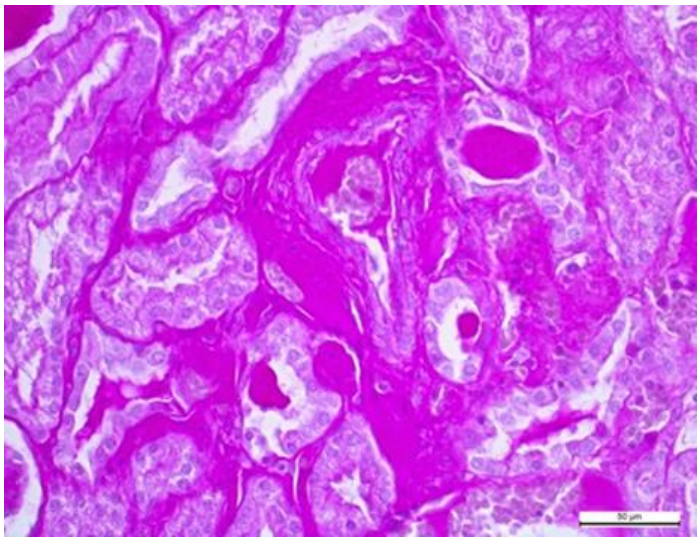

Fig. 40. Kidney. Perivascular edema with sharply sweating PAS-positive substances. PAS reaction. 400x.

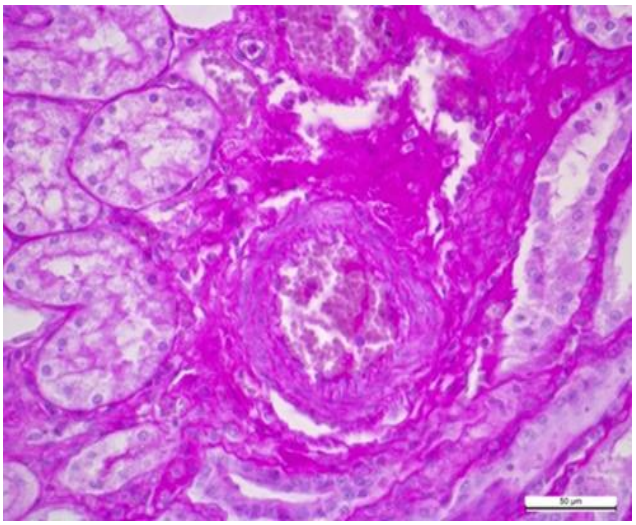

Fig. 41. Kidney. Perivasal edema. PAS reaction. 400x.

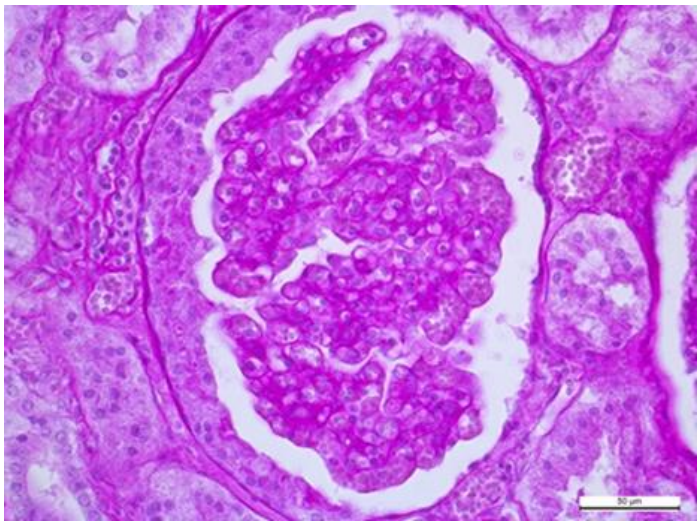

Fig. 42. Kidney. Diffuse proliferative glomerulonephritis. PAS reaction. 400x.

Thus, after the virus entered the body through the blood and lymphatic vessels, its reproduction took place in sensitive cells, accompanied by a cytopathic effect on leukocytes, macrophages, and endothelial cells. The virus caused necrosis of blood vessel endothelial cells, disorganization of small vessels' connective tissue structures, and total rhexis of lymphocytes. At the same time, a

large amount of the virus was released into the blood. That is why, after the virus entered the body of pigs, sharp hyperemia was clinically noted, along with an enlargement of regional lymph nodes in which there was an increased proliferation of lymphocytes and macrophages. The number of eosinophils in the blood increased too. Pathohistological examination revealed edema and vascular walls defibering, erythrocytosis, hyperemia, and serous hemorrhagic edema of lymph nodes. Additionally, lymphocyte necrosis, endothelial cell proliferation, mucoid and fibrinoid swelling of blood vessel walls were identified being the characteristic manifestations of ASF. After primary replication, the virus enters other organs, i.e., spleen, lungs, liver, kidneys, where it undergoes its secondary replication. The virus multiplies intensively, causing viremia, leukopenia, and lymphopenia, resulting from lymphocyte apoptosis. The ASF virus induces increased hematopoiesis in the bone marrow, but this is not enough to compensate for the loss of lymphocytes in the blood. There was a strong blood supply to the vessels in the lungs, activation of the alveolar epithelium, and a sharp violation of blood supply. Serous sweating and erythrocytes in the alveoli, alveolar dystrophy, bronchial epithelium were found in the lumens of the alveoli and the interstitial tissue.

Conclusion

The revealed macroscopic and microscopic changes in pigs are the characteristic features of acute ASF. The following signs were found in the lymph nodes and spleen: increased proliferation of lymphocytes, macrophages, endothelial cells, karyopyknosis, and karyorrhexis of lymphocytes, edema, fibrinoid swelling of vascular walls, hemorrhagic inflammation of the spleen. Systemic lesions of the vessel walls in all parenchymal organs were caused by stasis, thrombosis, plasmorrhagia, and hemorrhage. Disturbances of protein and lipid and carbohydrate metabolism are typical for this disease. Serous hemorrhagic pneumonia with sharp edema of interstitial tissue developed in the lungs. The development of hemorrhagic diathesis, tissue damage at the site of hemorrhage and hemostasis, hypoxia of parenchymal organs are the consequences of a sharp violation of hemodynamics caused by the African swine fever virus.

References

Beltrán-Alcrudo, D., Arias, M., Gallardo, C., Kramer, S. & Penrith, M. L. (2017). African swine fever: detection and diagnosis – A manual for veterinarians. FAO Animal Production and Health Manual No. 19. Rome. Food and Agriculture Organization of the United Nations (FAO).

Beltran-Alcrudo, D., Falco, J. R., Raizman, E. et al. (2019). Transboundary spread of pig diseases: the role of international trade and travel. BMC Vet Res 15, 64.

Blome, S., Gabriel, C., Beer, M. (2013). Pathogenesis of African swine fever in domestic pigs and European wild boar. Virus Res, 173(1), 122-30.

Cwynar, P., Stojkov, J., Wlazlak, K. (2019). African Swine Fever Status in Europe. Viruses, 11(4), 310.

De la Torre, A., Bosch, J., Iglesias, I., Muñoz, M. J., Mur, L., Martínez-López, B., Martínez, M., Sánchez-Vizcaíno, J. M. (2015). Assessing the Risk of African Swine Fever Introduction into the European Union by Wild Boar. Transbound Emerg Dis, 62(3), 272-9.

Dee, S. A, Bauermann, F. V., Niederwerder, M. C., Singrey, A., Clement, T., de Lima, M., Long, C., Patterson, G., Sheahan, M. A., Stoian, A. M. M., Petrovan, V., Jones, C. K., De Jong, J., Ji, J., Spronk, G. D., Minion, L., Christopher-Hennings, J., Zimmerman, J. J., Rowland, R. R. R., Nelson, E., Sundberg, P., Diel, D. G. (2018). Survival of viral pathogens in animal feed ingredients under transboundary shipping models. PLoS One. 13 (3):e0194509.

Dixon, L. K., Chapman, D. A., Netherton, C. L., Upton, C. (2013). African swine fever virus replication and genomics. Virus Res. Apr;173 (1):3-14.

Ezema, W. S., Aba Adulugba, E. P., Luther, J. N. and Okoye, J. O. A. (2011). Histopathological Changes Associated with Epizootic of African Swine Fever in Nigeria. Journal of Animal and Veterinary Advances, 10:1829-1832.

Flannery, J., Moore, R., Marsella, L., Harris, K., Ashby, M., Rajko-Nenow, P., Roberts, H., Gubbins, S., Batten, C. (2020). Towards a Sampling Rationale for African Swine Fever Virus Detection in Pork Products. Foods. 9 (9):1148.

Food and Agriculture Organization of the United Nations Statistics [FAOSTAT], http://www.fao.org/faostat/en/#home (2019).

Galindo, I., Alonso, C. (2017). African Swine Fever Virus: A Review. Viruses. May 10;9(5):103.

Ge, S., Li, J., Fan, X., Liu, F., Li, L., Wang, Q., Ren, W., Bao, J., Liu, C., Wang, H., Liu, Y., Zhang, Y., Xu, T., Wu, X., Wang, Z. (2018). Molecular Characterization of African Swine Fever Virus, China, 2018. Emerg Infect Dis. 24 (11) :2131-2133.

Gómez-Villamandos, J. C., Bautista, M. J., Sánchez-Cordón, P. J., Carrasco, L. (2013). Pathology of African swine fever: the role of monocyte-macrophage. Virus Res. 173 (1):140-9.

Kiceli, D. (1962). Prakticheckaja mikpotehnika i gictohimija. Budapesht (in Russian).

Kim, H. J., Lee, M. J., Lee, S. K., Kim, D. Y., Seo, S. J., Kang, H. E., Nam, H. M. (2019). African Swine Fever Virus in Pork Brought into South Korea by Travelers from China, August 2018. Emerg Infect Dis. 25 (6):1231-1233.

Makarov, V. V. (2018). African swine fever, Rossijskij veterinarnyj zhurnal (Russian veterinary journal). No. 6, pp. 15–19.

Mazloum, A., Igolkin, A. S., Vlasova, N. N., Romenskaya, D.V. (2019). African swine fever virus: use of genetic markers in analysis of its routes of spread. Veterinary Science Today. (3):3-14.

Merkulov, G. A. (1969). Kurc patologicheckoj tehniki. L. (in Russian).

Mur, L., Martínez-López, B., Sánchez-Vizcaíno, J. M. (2012). Risk of African swine fever introduction into the European Union through transport-associated routes: returning trucks and waste from international ships and planes. BMC Vet Res. 8:149.

Pautienius, A., Grigas, J., Pileviciene, S., Zagrabskaite, R., Buitkuviene, J., Pridotkas, G., Stankevicius, R., Streimikyte, Z., Salomskas, A., Zienius, D., Stankevicius, A. (2018). Prevalence and spatiotemporal distribution of African swine fever in Lithuania, 2014-2017. Virol J. 15 (1):177.

Pejsak, Z., Niemczuk, K., Frant, M., Mazur, M., Pomorska-Mól, M., Ziętek-Barszcz, A., Bocian, Ł., Łyjak, M., Borowska, D., Woźniakowski, G. (2018). Four years of African swine fever in Poland. New insights into epidemiology and prognosis of future disease spread. Pol J Vet Sci. 21 (4):835-841.

Pejsak, Z., Truszczyński, M., Niemczuk, K., Kozak, E., Markowska-Daniel, I. (2014). Epidemiology of African Swine Fever in Poland since the detection of the first case. Pol J Vet Sci. 17(4):665-72.

Rodríguez-Bertos, A., Cadenas-Fernández, E., Rebollada-Merino, A., Porras-González, N., Mayoral-Alegre, F. J., Barreno, L., Kosowska, A., Tomé-Sánchez, I., Barasona, J. A., Sánchez-Vizcaíno, J. M. (2020). Clinical Course and Gross Pathological Findings in Wild Boar Infected with a Highly Virulent Strain of African Swine Fever Virus Genotype II. Pathogens. 9(9):688.
Salguero, F. J. (2020). Comparative Pathology and Pathogenesis of African Swine Fever Infection in Swine. Front Vet Sci. 7:282
Sánchez-Cordón, P. J., Nunez, A., Neimanis, A., Wikström-Lassa, E., Montoya, M., Crooke, H., Gavier-Widén, D. (2019). African Swine Fever: Disease Dynamics in Wild Boar Experimentally Infected with ASFV Isolates Belonging to Genotype I and II. Viruses. 11 (9):852.
Sanchez-Cordon, P. J., Romero-Trevejo, J. L., Pedrera, M., Sanchez-Vizcaino, J. M., Bautista, M. J., Gomez-Villamandos, J. C. (2008). Role of hepatic macrophages during the viral hemorrhagic fever induced by African Swine Fever Virus. Histol Histopathol. 23:683–91.
Sánchez-Vizcaíno, J. M., Mur, L., Gomez-Villamandos, J. C., Carrasco, L. (2015). An update on the epidemiology and pathology of African swine fever. J Comp Pathol. 152(1):9-21.
Sunwoo, S. Y., Pérez-Núñez, D., Morozov, I., Sánchez, E. G., Gaudreault, N. N., Trujillo, J. D., Mur, L., Nogal, M., Madden, D., Urbaniak, K., Kim, I. J., Ma, W., Revilla, Y., Richt, J. A. (2019). DNA-Protein Vaccination Strategy Does Not Protect from Challenge with African Swine Fever Virus Armenia 2007 Strain. Vaccines (Basel). Jan 28;7 (1):12.
Tulman, E. R, Delhon, G. A, Ku, B. K, Rock, D. L. (2009). African swine fever virus. Curr Top Microbiol Immunol. 328:43-87.
Uikli B. (1975). Elektronnaya mikroskopiya dlya nachinayuschih. Moscow. Mir (in Russian).
Zakaryan, H., Cholakyans, V., Simonyan, L. et al. (2015). A study of lymphoid organs and serum proinflammatory cytokines in pigs infected with African swine fever virus genotype II. Arch Virol 160, 1407–1414.

Citation:
Shchebentovska, O., Zaytsev, O., Tybinka, A., Lozhkina, O., Kupnevska, M., Lytvynenko, S. (2021). Pathological and pathohistological characteristics of African swine fever in the western region of Ukraine. Ukrainian Journal of Ecology, 11 (4), 18-29.